Influence of chemical disorder on wavefunctions and optical transition rates in one-dimensional systems

1989 J. Phys.: Condens. Matter 1 6633

(http://iopscience.iop.org/0953-8984/1/37/011)

J. Phys.: Condens. Matter 1 (1989) 6633–6647. Printed in the UK

Influence of chemical disorder on wavefunctions and optical transition rates in one-dimensional systems

H Carruzzo, K Maschke and N Vandeventer
Ecole Polytechnique Fédérale de Lausanne, Institut de Physique Appliquée, CH-1015 Lausanne, Switzerland

Received 25 November 1988, in final form 30 January 1989

Abstract. We investigate the influence of chemical disorder on wavefunctions and optical transition rates in a one-dimensional (1D) alloy A_xB_{1-x}. The Schrödinger equation is solved for real-space A and B potentials. Even for large disorder, where the states are localised over only a few lattice sites, the calculated spectral function shows a strong dependence on the energy E and the k-vector, which can be understood as a remnant of the virtual-crystal band structure. The dependence of the optical matrix elements on the energies of the initial and final states is explained by that of the overlaps of the respective eigenfunctions in real and in k-space. For large disorder, the overlap in real space between valence states and conduction states near the gap becomes small, and in consequence the corresponding optical transitions are suppressed. The results are compared with the coherent potential approximation (CPA). It is found that even in our case of 1D disorder, which is the most difficult for CPA, the general behaviour of the transition matrix elements can be understood within the single-site CPA.

1. Introduction

In disordered systems the electron wavefunctions are usually characterised by their localisation properties. Thus it is now generally accepted that 1D and 2D disorder leads to spatially localised eigenfunctions, whereas for 3D disorder the eigenstates may be extended or localised, depending on the amount of disorder and on the energy (Abrahams *et al* 1979). Moullet *et al* (1985) and Ingers *et al* (1988) have shown recently that this description of the wavefunctions is insufficient. In particular it does not allow us to understand the energy dependence of optical matrix elements, which are strongly influenced by the phases of the involved wavefunctions. This is similar to the situation found for translation-invariant ordered crystals, where the optical matrix elements depend essentially on the phases of the Bloch eigenfunctions, which give rise to the k-selection rule. Moullet *et al* (1985) have shown that the energy dependence of the phase correlations of the wavefunctions in disordered systems remains very similar with respect to the ordered crystal, and they have therefore suggested that the k-selection rule for optical transitions remains important even when the eigenfunctions are localised over only a few sites, and that it weakens only gradually with increasing disorder. This has been confirmed by the numerical calculations of Ingers *et al* (1988). Their calculations have, however, only been done for the case of a rather academic disorder, where the stochastic parameters responsible for the disorder, which were either the diagonal elements in an Anderson Hamiltonian or the depths of the atomic potentials positioned

0953-8984/89/376633 + 15 $02.50

at the lattice sites of a regular lattice, were distributed according to a rectangular distribution function.

In the present paper we investigate the situation for the more realistic case of chemical disorder A_xB_{1-x}. As Ingers *et al* (1988) we restrict ourselves to the case of disordered 1D chains, which are not only interesting in themselves but are also sufficient for the discussion of the specific properties of chemical disorder, as long as we are only interested in its principal characteristics. Since it is difficult to study inter-band correlations within a two-band Anderson model (see Ingers *et al* 1988), we solve the Schrödinger equation for real-space A and B potentials. It will be shown not only that the k-selection rule does not immediately lose its significance in the presence of chemical disorder, as might be expected from the results of Ingers *et al* (1988), but also that it remains important up to very large disorder, where the electron states are essentially separated in A and B states and localised over only a very small number of lattice sites. Further, we give evidence for a spatial correlation between states belonging to different bands. This is in contrast to the findings of Ingers *et al* (1988) for the case of continuous disorder, for which no particular spatial inter-band correlations could be observed.

The numerical results are compared with the predictions of the single-site CPA method (Soven 1967, 1969, Velicky *et al* 1968, Velicky 1969, Abe and Toyozawa 1981). We find that the CPA explains the principal effects of chemical disorder, excepting the tail region near the band edges. Even in the most critical case of 1D disorder, where it is less adequate, it provides a good overall description of the behaviour of the one-electron states, as well as the optical spectra. This is encouraging since the CPA approach is much more reliable in 2D and 3D, where direct calculations of the optical properties of disordered systems become very difficult, if not impossible.

2. Numerical approach

Our calculations are based on the Hamiltonian

$$H = -\Delta + \sum_{n=1}^{N} a_n v(x - na). \tag{1}$$

It describes a chain of N atoms, in which the atoms are positioned on the sites of a regular 1D lattice with lattice constant a. The parameter a_n distinguishes between A and B atoms, i.e. it oscillates between two possible values

$$a_n = \begin{cases} a_0 + W & \text{for A atoms} \\ a_0 - W & \text{for B atoms} \end{cases} \tag{2}$$

which are statistically distributed over the chain according to the concentrations x and $1 - x$. For simplicity we describe the spatial dependence of the atom potentials by Gaussians

$$v(x) = -(\alpha/\pi)^{1/2}\exp(-\alpha x^2). \tag{3}$$

The Schrödinger equation can be solved easily in a basis set of plane waves for either periodic or anti-periodic boundary conditions. In our calculations we take a sufficiently large disorder, i.e. a sufficiently large W, such that for the chosen chain length of N atoms and within the considered energy range, the localised eigenstates of the Hamiltonian (1) are not influenced by the type of boundary conditions, and therefore are representative of an infinite disordered chain.

The eigenstates are given by the eigenvalues E_i and the eigenfunctions ψ_i. For periodic boundary conditions we obtain

$$\psi_i(x) = \sum_n c_n^i \exp(\mathrm{i}K_n x) \tag{4}$$

with $K_n = (2\pi/Na)n$ and $n = -M, \ldots, -1, 0, 1, \ldots, M$. By replacing the a_n in equation (1) by their average value a_0 (see equation (2)), we obtain the virtual-crystal Hamiltonian. In this case the eigenstates are given by the band structure $E^l(k)$ and the Bloch eigenfunctions $\psi_k^l(x)$, where l is the band index and k is limited to the first Brillouin zone, i.e.

$$-\pi/a < k \leqslant \pi/a.$$

Defining an energy resolution Δ through the filter function

$$\delta^\Delta(E) = \begin{cases} 1 & \text{for } |E| < \Delta/2 \\ 0 & \text{otherwise} \end{cases} \tag{5}$$

we can calculate the density of states

$$g(E) = \left\langle\!\!\left\langle \sum_n \delta^\Delta(E - E_n) \right\rangle\!\!\right\rangle \tag{6}$$

and the participation number

$$p(E) = \frac{1}{g(E)} \left\langle\!\!\left\langle \sum_n \frac{1}{\sum_i (q_i^n)^2} \delta^\Delta(E - E_n) \right\rangle\!\!\right\rangle \tag{7}$$

which measures the number of sites covered by the wavefunctions. Here q_i^n is the charge of state n at atom i

$$q_i^n = \int_{(i-\frac{1}{2})a}^{(i+\frac{1}{2})a} |\psi_n(x)|^2 \, \mathrm{d}x. \tag{8}$$

The brackets $\langle\!\langle \ldots \rangle\!\rangle$ indicate configurational averaging. The average optical matrix element for a given photon energy $\hbar\omega$ and a given final-state energy E_f is obtained as

$$M(E_f, \hbar\omega) = \frac{1}{g(E_i)g(E_f)} \delta^\Delta(E_i - E_f + \hbar\omega) \times \left\langle\!\!\left\langle \sum_{n,m} \delta^\Delta(E_m - E_f)\delta^\Delta(E_n - E_i) \, |\langle n|p|m\rangle|^2 \right\rangle\!\!\right\rangle \tag{9}$$

with

$$\langle n|p|m\rangle = \sum_s c_s^{n*} c_s^m K_s. \tag{10}$$

For comparison we also calculate the spatial overlap between the initial and final states in equation (9)

$$O(E_f, \hbar\omega) = \frac{1}{g(E_i)\, g(E_f)} \delta^\Delta(E_i - E_f + \hbar\omega) \times \left\langle\!\!\left\langle \sum_{n,m} \delta^\Delta(E_m - E_f)\delta^\Delta(E_n - E_i) o_{nm}^2 \right\rangle\!\!\right\rangle \tag{11}$$

with

$$o_{nm} = \sum_i (q_i^n)^{1/2} (q_i^m)^{1/2}. \tag{12}$$

In order to study the influence of the disorder on the electron states, we expand the

localised eigenfunctions $\psi^i(x)$ in the basis of the Bloch eigenfunctions of the virtual crystal

$$\psi_i(x) = \sum_{l,k} c^i_{lk} \psi^l_k(x) \tag{13}$$

and calculate the spectral function

$$S(lk, E) = \sum_i \delta^\Delta(E - E_i)|c^i_{lk}|^2. \tag{14}$$

3. Coherent potential approximation approach

It is evident that it will be rather difficult to apply the numerical approach described above to 2D or 3D disordered systems, since the number of plane waves necessary to obtain convergence for the lowest bands increases with the power of the dimension. For this reason, and also because it would be satisfying to understand the general behaviour of the eigenstates in the presence of disorder in a more analytical way, we have tested the extent to which the single-site CPA (Soven 1967, 1969, Velicky *et al* 1968, Velicky 1969, Abe and Toyozawa 1981) is able to predict our numerical results. The CPA has the advantage that it is easily applicable to 2D and 3D systems, where it is even more reliable than in one dimension. It is also known that localised states in the band region are correctly treated within the single-site CPA. It fails, however, in the tail region, where the states are localised at specific clusters of atoms. Comparison between our numerical results and the CPA results will thus give evidence for the importance of such cluster states in this energy region.

The CPA has been extensively discussed in the literature. It has also been extended beyond the single-site approximation (Economou 1979, and references therein). For simplicity, we have, however, based our calculations of the density of states and of the spectral function on the original formulation of Soven (1969). In the following we briefly recall the general expressions that are necessary for our calculations, and refer the reader for further details to Soven (1969) and Velicky *et al* (1968).

Under the assumption that the disorder is sufficiently weak, such that inter-band interactions can be neglected, we start from the configurational average of the Green function for a single band l. In the CPA this is written as

$$\langle\langle G^{l+}(E)\rangle\rangle = \frac{1}{E - H^l_0 - \Sigma^l(E)} \tag{15}$$

where H^l_0 is the Hamiltonian operator that describes the band l of the virtual crystal and $\Sigma^l(E)$ is an energy-dependent complex self-energy. Calculating the diagonal matrix elements between the Bloch eigenfunctions of the virtual-crystal Hamiltonian we obtain for the spectral function for a given band l of the disordered system

$$\begin{aligned} S(lk, E) &= -(1/\pi)\,\mathrm{Im}\langle lk|\langle\langle G^{l+}(E)\rangle\rangle|lk\rangle \\ &= -(1/\pi)\,\mathrm{Im}\frac{1}{E - E^l(k) - \Sigma^l(E)}. \end{aligned} \tag{16}$$

The corresponding density of states $g^l(E)$ is

$$g^l(E) = [1/2\pi]\int \mathrm{d}k\, S(lk, E). \tag{17}$$

$\Sigma^l(E)$ is obtained from the condition that the average single-site t-matrix vanishes, if all

energies and potentials in the corresponding expression are shifted by $\Sigma^l(E)$, i.e. Σ^l must satisfy the condition

$$\langle\langle t^l \rangle\rangle = \sum_\alpha \frac{c_\alpha[v_\alpha - \Sigma^l(E)]}{1 - G_0^{l+}[E - \Sigma^l(E)][v_\alpha - \Sigma^l(E)]} = 0 \qquad \text{with } \alpha = \mathrm{A}, \mathrm{B}. \tag{18}$$

Here v_A and v_B are the potentials of the A and B atoms; c_A and c_B the respective concentrations, i.e. $c_\mathrm{A} = x$ and $c_\mathrm{B} = 1 - x$; and G_0^{l+} is the Green function for the lth band of the virtual crystal.

Under the assumption that the matrix elements $\langle lk|v_\alpha|lk'\rangle$ depend only weakly on k and k', we can replace them by their mean value

$$\begin{aligned} \langle lk|v_\mathrm{A}|lk'\rangle &\simeq (a_0 - W)\bar{v}^l =: \overline{v_\mathrm{A}}^l \\ \langle lk|v_\mathrm{B}|lk'\rangle &\simeq (a_0 - W)\bar{v}^l =: \overline{v_\mathrm{B}}^l \end{aligned} \tag{19}$$

with

$$\bar{v}^l = \overline{\langle lk|v|lk'\rangle} = \text{const.}$$

The bar indicates the averaging with respect to k and k'. It should be noted that the global phases of the wavefunctions are arbitrary. It can easily be seen that they will not influence the results discussed later. However, care must be taken that the phases do not enter the above average procedure. In order to obtain a meaningful average, one has to define a unique phase of the matrix elements, e.g. by taking the sign of the matrix element at $k = k' = 0$, or by averaging the absolute values. $\Sigma^l(E)$ is then obtained from

$$\langle lk|\langle\langle t^l\rangle\rangle|lk'\rangle = \sum_\alpha \frac{c_\alpha[\bar{v}_\alpha^l - \Sigma^l(E)]}{1 - \{[\bar{v}_\alpha^l - \Sigma^l(E)]a/2\pi\}\int \mathrm{d}q/[E^+ - E^l(q) - \Sigma^l(E)]} = 0 \qquad \alpha = \mathrm{A}, \mathrm{B}. \tag{20}$$

Equation (20) can be solved by numerical iteration.

The optical transition matrix elements will be analysed within the framework of the theory of Abe and Toyozawa (1981). Following Abe and Toyozawa we write for the optical absorption

$$I(E) = \iint \mathrm{d}E_1\, \mathrm{d}E_2\, \delta(E_2 - E_1 - E)S(E_1, E_2) \tag{21}$$

where the integration over E_1 (E_2) is taken over the occupied (unoccupied) states. The spectrum function $S(E_1, E_2)$ is given by

$$S(E_1, E_2) = \left\langle\!\!\left\langle \sum_n \langle nc|\,\delta(E_2 - H^\mathrm{c})\,|nc\rangle\,|\langle nc|\Pi|nv\rangle|^2\,\langle nv|\,\delta(E_2 - H^\mathrm{v})\,|nv\rangle \right\rangle\!\!\right\rangle \tag{22}$$

where Π is the dipole operator, $|nc\rangle$ ($|nv\rangle$) are the Wannier functions at site n of the conduction (valence) states, and H^c and H^v are the one-particle Anderson Hamiltonians for the conduction and valence bands, respectively.

The average matrix element for optical transitions between initial states at energy E_1 and final states at energy E_2 is then given by

$$M(E_1, E_2) = S(E_1, E_2)/g^\mathrm{v}(E_1)g^\mathrm{c}(E_2) \tag{23}$$

where g^v (g^c) is the valence (conduction) band density of states. For the calculation of $S(E_1, E_2)$ one assumes that $|\langle nc|\Pi|nv\rangle| = p = \text{const}$. In the following we put $p = 1$.

$S(E_1, E_2)$ can be expressed in terms of the Green function describing the valence (conduction) band

$$G^{v}(z_1) = 1/(z_1 - H^{v})$$
$$G^{c}(z_2) = 1/(z_2 - H^{c}). \tag{24}$$

We obtain

$$S(E_1, E_2) = (1/\pi^2)\langle\!\langle \langle nc|\operatorname{Im} G^{v}(E_1^+) C \operatorname{Im} G^{c}(E_2^+)\,|nv\rangle \rangle\!\rangle \tag{25}$$

with $E_1^+ = E_1 + i\varepsilon$ and $E_2^+ = E_2 + i\varepsilon$. The operator C is given by

$$C = \sum_n |nv\rangle\langle nc|. \tag{26}$$

Equation (25) can be rewritten using the configurational average of the two-particle Green function

$$K = \langle\!\langle \langle nc|G^{c} C G^{v}\,|nv\rangle \rangle\!\rangle. \tag{27}$$

We get

$$S(E_1, E_2) = [1/(2\pi i)^2][K(E_1^+, E_2^+) - K(E_1^-, E_2^+) - K(E_1^+, E_2^-) + K(E_1^-, E_2^-)]. \tag{28}$$

As shown by Abe and Toyozawa (1981), $K(z_1, z_2)$ can be calculated from

$$K(z_1, z_2) = \frac{R(z_1, z_2)}{1 - R(z_1, z_2) Q(z_1, z_2)} \tag{29}$$

with

$$Q(z_1, z_2) = \frac{\langle\!\langle t_n^{v}(z_1) t_n^{c}(z_2)\rangle\!\rangle}{1 + F^{v}(z_1)\langle\!\langle t_n^{v}(z_1) t_n^{c}(z_2)\rangle\!\rangle F^{c}(z_2)} \tag{30}$$

and

$$R(z_1, z_2) = (1/N) \sum_k F_k^{v}(z_1) F_k^{c}(z_2). \tag{31}$$

In the above equations $F_k^{\mu}(z)$, μ = v, c, is the diagonal matrix element of the virtual-crystal Green functions in the representation of the Bloch eigenfunctions, i.e.

$$F_k^{\mu}(z) = \langle k\mu|G_0^{\mu}(z)|k\mu\rangle \qquad \mu = \text{v, c}. \tag{32}$$

In the on-site approximation we obtain

$$\langle\!\langle t_n^{v}(z_1) t_n^{c}(z_2)\rangle\!\rangle = \sum_\alpha g_\alpha^{v}(z_1) g_\alpha^{c}(z_2) t_\alpha^{v}(z_1) t_\alpha^{c}(z_2) \qquad \alpha = \text{A, B} \tag{33}$$

with

$$t_\alpha^{\mu} = \frac{v_\alpha^{\mu} - \Sigma^{\mu}(E)}{1 - [v_\alpha^{\mu} - \Sigma^{\mu}(E)]\, F^{\mu}[v_\alpha^{\mu} - \Sigma^{\mu}(E)]}. \tag{34}$$

In (33), $g_A^{\mu}(E)$ and $g_B^{\mu}(E)$ are the partial density of states, which measure the contribution of A and B states, respectively, such that

$$g^{\mu}(E) = g_A^{\mu}(E) + g_B^{\mu}(E) \qquad \mu = \text{v, c}. \tag{35}$$

In (34), $F^{\mu}(z)$ is given by

$$F^{\mu}(z) = (1/N) \sum_k F_k^{\mu}(z) = \frac{1}{N} \sum_k \frac{1}{z - E^{\mu}(k) - \Sigma^{\mu}(z)}. \tag{36}$$

The densities $g_A^{\mu}(E)$ ($g_B^{\mu}(E)$) are calculated according to Velicky *et al* (1968). We obtain

$$g_\alpha^{\mu}(E) = -\frac{c_\alpha}{\pi} \operatorname{Im} F^{\mu}(z) \left(\frac{1}{1 - [\varepsilon_\alpha^{\mu} - \Sigma^{\mu}(E)] F^{\mu}(z)}\right)\Bigg|_{z = E + i\varepsilon}. \tag{37}$$

For the evaluation of $g_\alpha^{\mu}(E)$ we note that in our case of chemical disorder the disorder

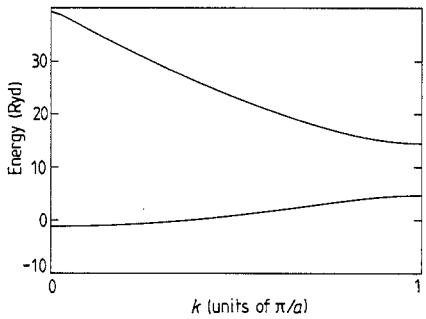

Figure 1. Band structure of the virtual crystal.

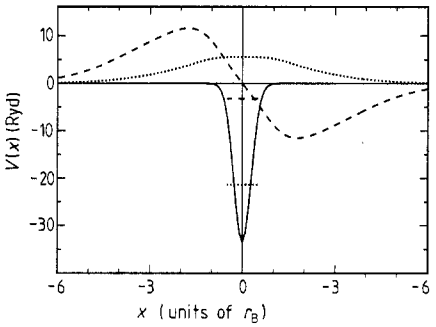

Figure 2. Eigenstates of the single atom potential. The atom potential is represented by the full curve. The eigenfunctions (arbitrary units) and eigenenergies are given by the dotted and broken curves.

in the valence and conduction bands is spatially correlated. In other words, the matrix elements

$$\varepsilon_n^{\mathrm{v}} = \langle nv|H^{\mathrm{v}}|nv\rangle$$

and

$$\varepsilon_n^{\mathrm{c}} = \langle nc|H^{\mathrm{c}}|nc\rangle$$

fluctuate in the same sense at each site n around their mean values ε^{v} and ε^{c}, i.e.

$$\varepsilon_n^{\mathrm{c}} - \varepsilon^{\mathrm{c}} = \beta(\varepsilon_n^{\mathrm{v}} - \varepsilon^{\mathrm{v}}) \tag{38}$$

with $\beta > 0$.

4. Numerical results

For our calculations we have used the following parameters: $a = 1r_{\mathrm{B}}$, $\alpha = 6.25r_{\mathrm{B}}^2$, $a_0 = 23.75$, $N = 60$, $x = 0.5$. The configurational average includes 20 samples. The number of plane waves in our basis set is equal to 361, i.e. we take $M = 180$ in equation (4). With this choice the eigenstates in the energy range of the first two bands of the virtual crystal are fully converged, independent of the disorder. Two strengths of disorder were considered: $W = 1.75$ (weak disorder) and $W = 2.75$ (strong disorder). These parameters scale with the lattice constant, as shown by Ingers *et al* (1988). The energy resolution for the calculated densities of states is $\Delta = 1$ Ryd; for the other quantities we have given the results for $\Delta = 0.5$ Ryd. The band-structure energies are given with respect to the average potential.

In principle the calculated eigenstates will depend slightly on the chosen boundary conditions (periodic or anti-periodic), depending on their localisation properties. We have carefully controlled that for the above energy resolution the boundary conditions do not influence the results presented. In fact, in the considered energy range the individual eigenstates already turn out to be independent of the boundary conditions chosen. This is true even for the participation number of individual states, which in this respect is the most critical of the quantities presented. We find that only states well above the lower band edge of the second band with participation numbers of the order of 20–30 start to become slightly dependent on the boundary conditions.

The virtual-crystal band structure ($W = 0$) is shown in figure 1. For comparison we show in figure 2 the eigenstates of the single Gaussian potential that corresponds to the

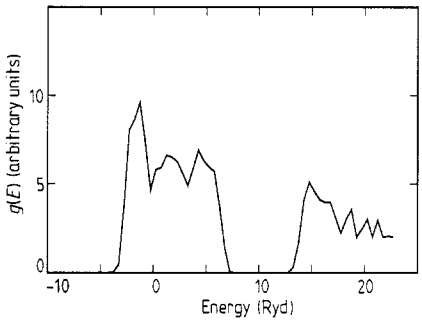

Figure 3. Density of states for weak disorder ($W = 1.75$, $\Delta = 1$).

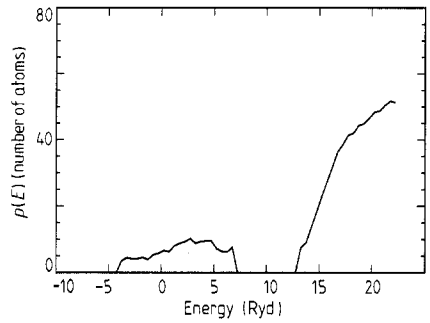

Figure 4. Participation number (weak disorder).

virtual crystal. The Gaussian potential has two bound eigenstates. The lowest one has even symmetry and is well separated in energy from the second one, which has odd symmetry. It is evident from figure 2 that the band with lowest energy can be described within a single orbital tight-binding model. This is not the case for the bands at higher energy, since already the second bound state is very close to the continuum. It can therefore be expected that these bands will rapidly become free-electron-like, i.e. independent of the potential and of the disorder. This general picture is in agreement with the band structure (figure 1) and also with our results for the alloy system, which are given in figures 3–7 for the case of weak disorder, and in figures 8–12 for the case of strong disorder.

We first discuss the case of weak disorder. The density of states is shown in figure 3. Besides the broadening of the $1/\sqrt{E}$ singularities at the band edges it still resembles that of the virtual crystal. As already suggested above, the conduction band is much less affected by the disorder than the valence band. The oscillations on the high-energy side are due to our method of calculation. Our supercell approach is only valid for sufficiently strong disorder, where the states are scattered between the energy intervals of width Δ. In the case of weak disorder it gives rise to fluctuations in the region of low density. With our parameters ($\Delta = 1$ Ryd, $N = 60$), these spurious oscillations around the true density of states only become important in the high-energy region of the conduction band. Since we are mainly interested in the optical transitions involving conduction band states close to the gap, we do not correct for this effect.

The energy dependence of the participation number is shown in figure 4. Again the disorder affects mostly the valence band, where the electronic states are localised over 5–10 sites. In the conduction band only states near the band edge are strongly localised; states away from the band edge become rapidly delocalised and extend practically over the periodicity volume of 60 atoms. As mentioned before, the extended eigenstates in this energy range become dependent on the boundary conditions, and are therefore excluded from our discussion.

In figure 5 we show the spectral function (equation (14)) as a function of the energy of the localised states and of the k-vector of the unperturbed Bloch eigenfunctions of the virtual crystal. The results are given in the extended zone scheme, i.e. the first Brillouin zone corresponds to the unperturbed valence states, the second to the unperturbed conduction states. The principal effect of the disorder is an energy-dependent broadening of the spectral function of the disordered alloy with respect to that of the ordered virtual crystal. As already seen from the density of states and the participation number, the conduction band states are the less affected by the disorder. The maximum

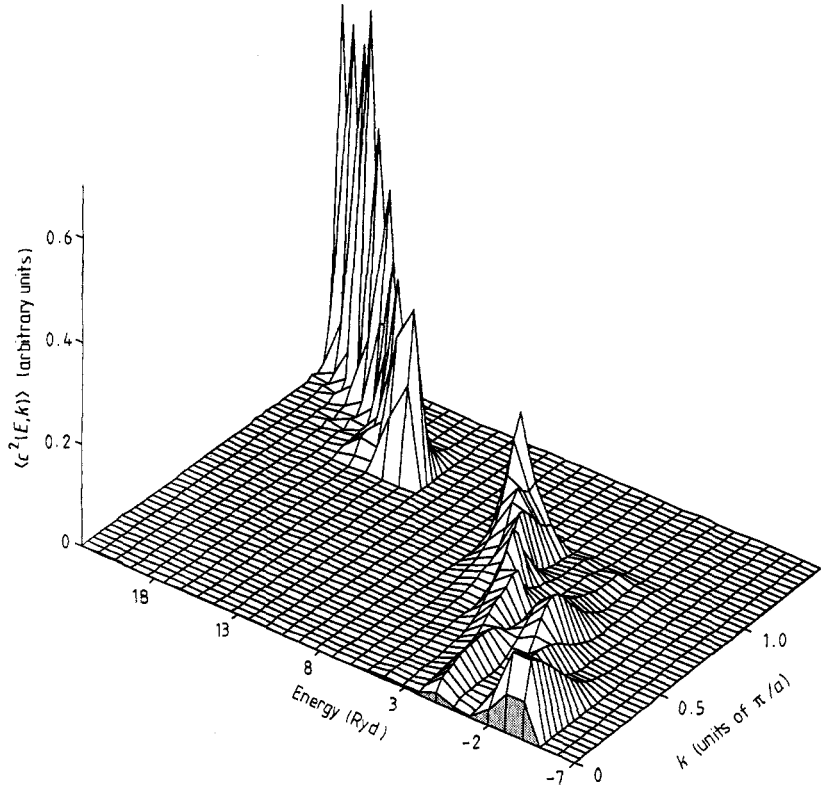

Figure 5. Spectral function (weak disorder).

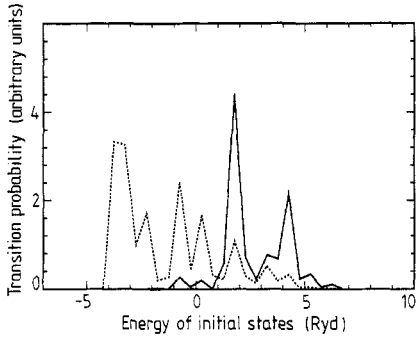

Figure 6. Optical matrix elements and spatial overlaps; the final-state energy (13–13.5 Ryd) is chosen close to the conduction band edge (weak disorder).

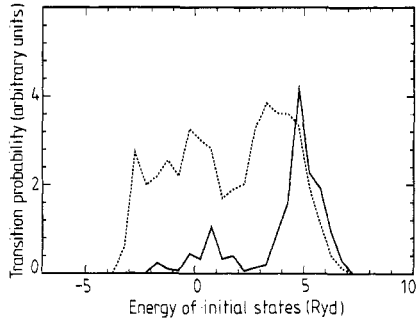

Figure 7. Optical matrix elements and spatial overlaps; the final-state energy (14–14.5 Ryd) is chosen higher in the conduction band (weak disorder).

of the spectral function follows an $E(k)$ relation, which resembles that of the virtual crystal. The result is very similar to the result presented by Ingers *et al* (1988) for continuous disorder. In the valence band we find, however, somewhat more structure, which indicates the beginning of a splitting of the valence band into two bands with predominantly A or B character.

The dependences of the calculated optical matrix elements and of the corresponding spatial overlaps on the energy of the initial states are shown in figures 6 and 7. The results

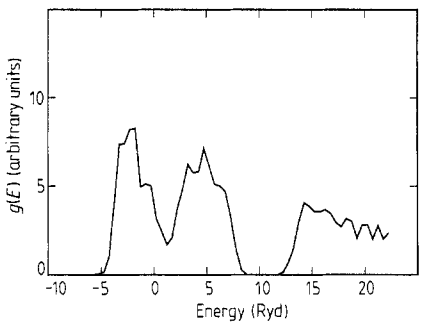

Figure 8. Density of states for strong disorder ($W = 2.75$, $\Delta = 1$).

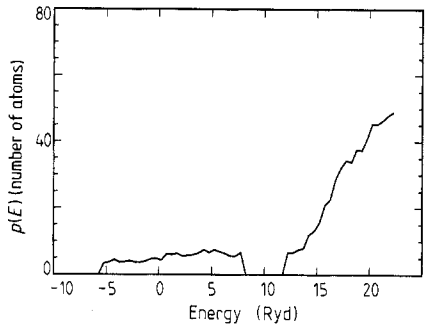

Figure 9. Participation number (strong disorder).

are given for two final energies, close to the conduction band edge (figure 6) and somewhat higher in the conduction band (figure 7). It is seen that the energy dependence of the optical matrix elements cannot be explained by the variation of the spatial overlap between initial and final states. For final states close to the conduction band minimum (figure 6) the energy dependence of the matrix elements becomes quite complicated. We find two maxima, one near the upper valence band edge at about 4 Ryd and the other even more pronounced inside the band at about 2 Ryd. Comparison with the spectral function (figure 5) and the spatial overlap given in figure 6 shows that the relative weight of the two maxima is essentially due to the behaviour of the latter, whereas the low transition probability for initial states with $E < 1$ Ryd is explained by the behaviour of the spectral function. The oscillatory behaviour of the spatial overlap indicates a significant spatial correlation between states at the conduction band edge and valence states.

The relative importance of the two peaks is reversed, when we consider transitions towards final states somewhat higher in energy (figure 7). In this case the overlap becomes more uniform and the energy dependence of the matrix elements is essentially explained by the overlap of initial and final states in k-space, i.e. the spectral function.

For stronger disorder the valence band splits into two bands with predominantly A or B character (figure 8) and the states become more localised (figure 9). The splitting into two bands is very niclely seen from the spectral function (figure 10). The two maxima of the spectral function in the valence band region again follow separately an $E(k)$ relation. The somewhat smaller dispersion of the band at lower energy can be attributed to the fact that the localisation of the atomic states increases with the depth of the atomic potential.

The energy dependence of the optical matrix elements and of the corresponding spatial overlaps is shown in figure 11 for final-state energies close to the conduction band edge, and in figure 12 for final states somewhat higher in the conduction band. The behaviour of the spatial overlap indicates that states near the conduction band edge are predominantly localised on the more attractive atoms (A atoms). This leads to the small (large) overlap with the valence states of type B (A).

5. CPA results

As already mentioned, the CPA method should work best for the lowest band ('valence band'), for which equation (19) is a good approximation. We therefore present first our

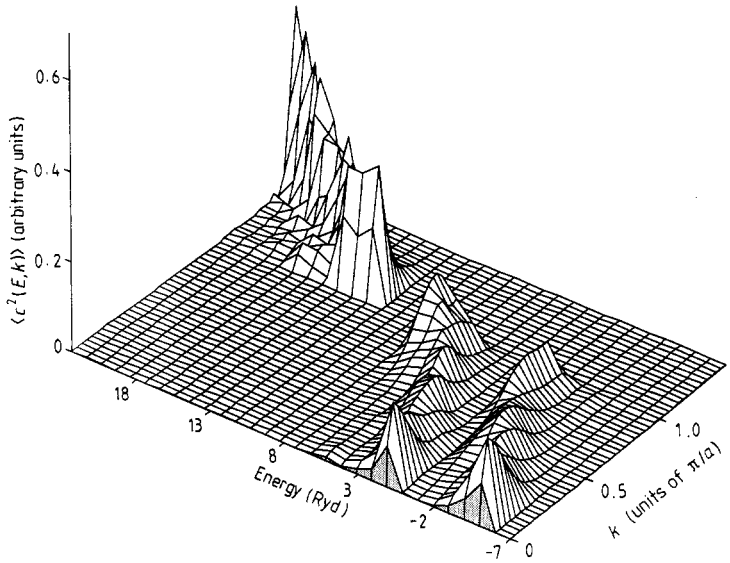

Figure 10. Spectral function (strong disorder).

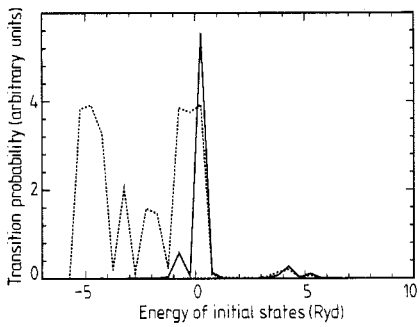

Figure 11. Optical matrix elements and spatial overlaps; the final-state energy (12–12.5 Ryd) is chosen close to the conduction band edge (strong disorder).

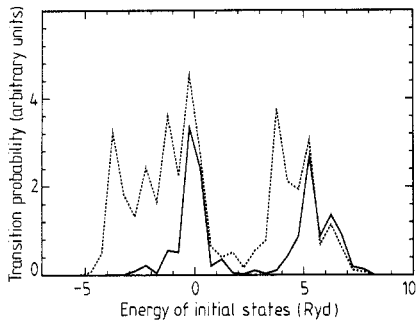

Figure 12. Optical matrix elements and spatial overlaps; the final-state energy (13.5–14 Ryd) is chosen higher in the conduction band (strong disorder).

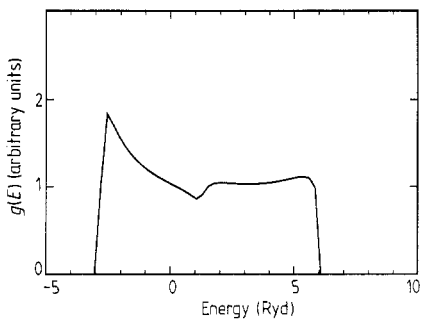

Figure 13. CPA, weak disorder; density of states for the valence band.

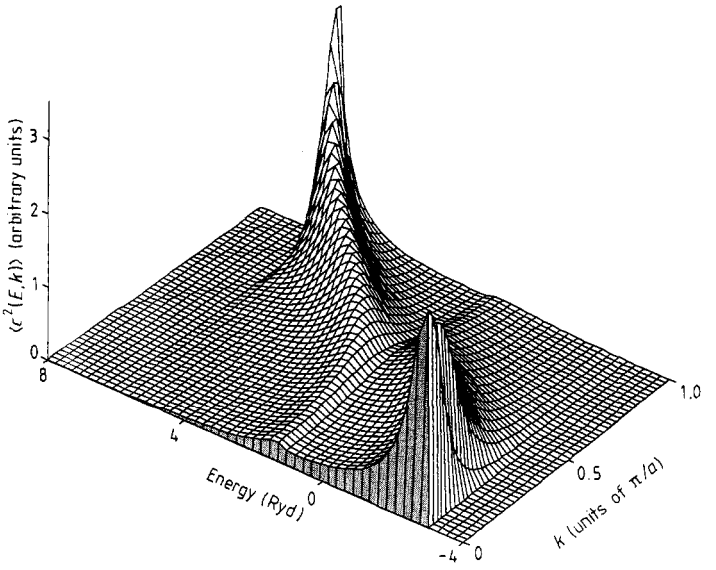

Figure 14. CPA, weak disorder; spectral function for the valence band.

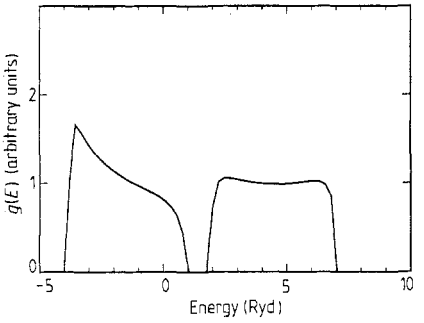

Figure 15. CPA, strong disorder; density of states for the valence band.

CPA results for the valence band of our model described in the previous section. The band structure of the virtual crystal as well as the matrix element of the single Gaussian between the virtual-crystal eigenfunctions (see equation (19)) are calculated numerically. For the matrix element we obtain $\bar{v}^l = 1.09 \pm 0.14$ Ryd; the approximation by its average value is thus reasonable. The other parameters remain the same as in the previous section. In figures 13 and 14 we show the results for the density of states and the spectral function for the case of weak disorder, and in figures 15 and 16 for the case of strong disorder. Comparison with the respective exact numerical results in figures 3, 5, 8 and 10 shows that the CPA method gives a quite satisfactory overall description of the effects of chemical disorder on the density of states as well as on the spectral function. As expected, the single-site CPA fails, however, in the tail regions near the band edges, in which the states are localised at small specific clusters. In principle, this can be corrected for by using the cluster CPA (see e.g. Eggarter and Troper 1987).

As already mentioned above, equation (19) is less justified for the description of the conduction band of our numerical model. Since in the present work we are only interested in the general ability of the CPA method to describe the dependence of the optical matrix elements on the initial- and final-state energy, we have applied the CPA to the simpler case of a two-band Anderson Hamiltonian with nearest-neighbour interaction V and

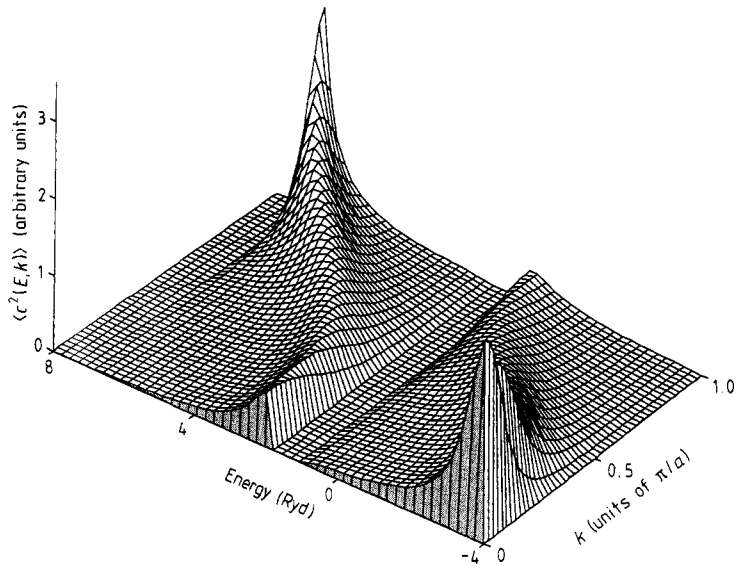

Figure 16. CPA, strong disorder; spectral function for the valence band.

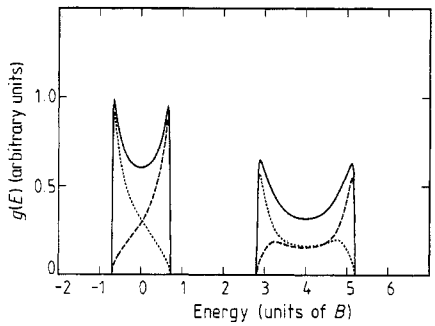

Figure 17. CPA model, weak disorder; model density of states for valence and conduction band, as well as partial density of states on A and B atoms.

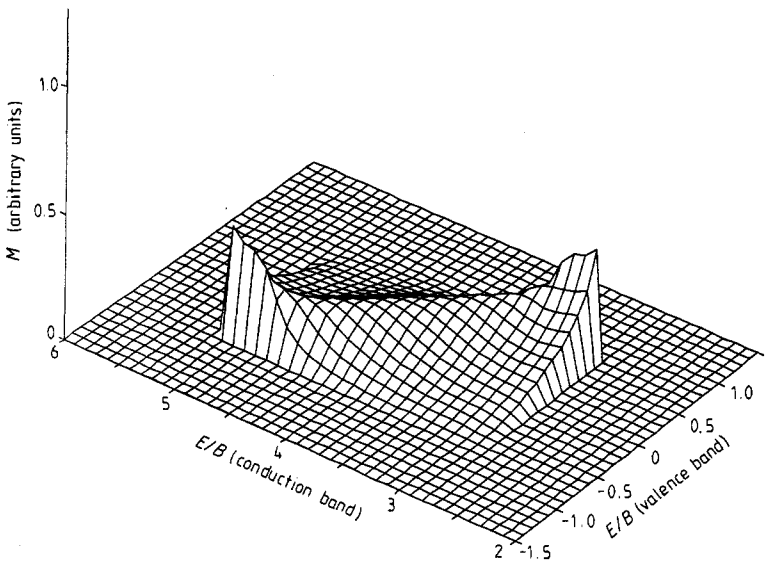

Figure 18. CPA model, weak disorder; optical matrix elements as a function of the initial- and final-state energies.

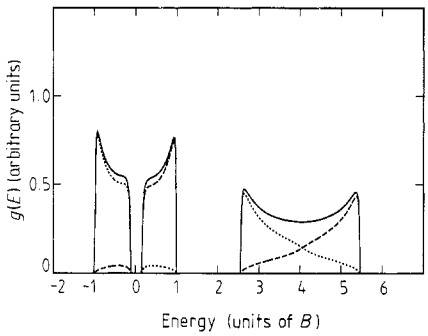

Figure 19. CPA model, strong disorder; model density of states for valence and conduction band, as well as partial density of states on A and B atoms.

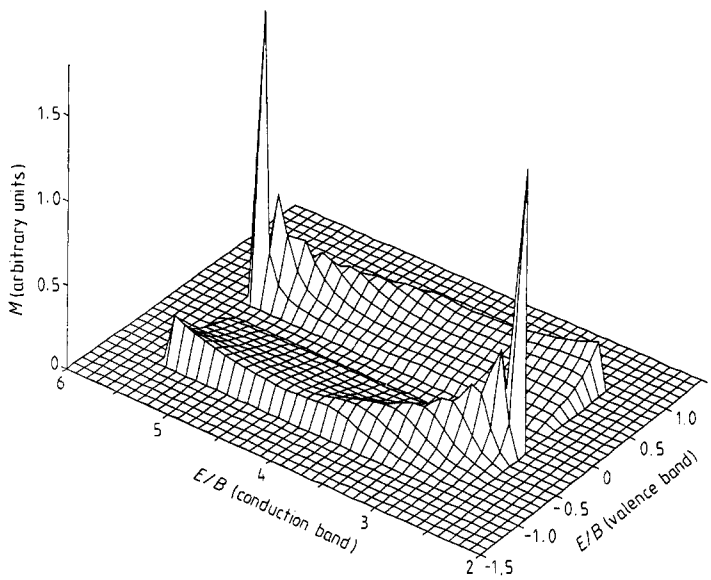

Figure 20. CPA model, strong disorder; optical matrix elements as a function of the initial- and final-state energies.

diagonal chemical disorder W. The parameters describing the virtual crystal are $V = -0.5B$ for the valence band, and $V = 1B$ for the conduction band. B defines the chosen energy units and thus does not influence the results. The centres of the two bands are placed at $\varepsilon^v = 0$ and $\varepsilon^c = 4B$, respectively. The dispersion of each band is thus given by a single cosine. The diagonal disorder is described by the fluctuations of amplitude $W/2$ around ε^v and ε^c. Since the disorder effects scale with the band widths we can reduce the number of parameters and take the same W for both bands.

Similar to the numerical calculations discussed in the previous section we present the results for two degrees of disorder, $W = 0.25B$ (weak disorder) and $W = 0.55B$ (strong disorder). The results for weak disorder are given in figures 17 and 18, and the results for stronger disorder in figures 19 and 20. Under the simplifying assumptions of the Anderson model the densities of states (figures 17 and 19) become symmetric with respect to the corresponding band centres. In agreement with the previous results, increasing disorder leads to a splitting of the two bands. We have also given the individual contributions of the A and B states to the total densities of states, which can be easily calculated in the present simplified CPA approach (see equation (37)). It is seen that in

fact the two contributions are separated in energy, such that low-energy states in each band are localised on the A atoms, whereas high-energy states in each band are localised on the less attractive B atoms. We emphasise that this is not a disorder effect, but is already observed in the ordered AB crystal.

The dependence of the optical matrix element on the energies of the initial and final states is shown in figures 18 and 20. With the exception of transitions involving states very close to the band edges, the CPA results are in good qualitative agreement with the numerical results discussed in the previous section. This shows that not only the energy dependence of the spectral function but also that of the spatial overlap, which are both needed for a correct description of the behaviour of the matrix elements, can be understood within the CPA approach.

6. Conclusions

We have investigated the influence of chemical disorder on the wavefunctions and on the optical transition matrix elements. Our numerical study shows that the dependence of the optical transition rates on the initial- and final-state energies can be understood from the localisation properties of the eigenfunctions in real space and in k-space. The optical matrix elements depend on the overlap of the involved functions in real space and, which is as important, also on their overlap in k-space. The dependence of the latter on the energy of the states is a consequence of the behaviour of the spectral function, which for weak disorder follows an $E(k)$ relation close to that of the virtual crystal. For strong disorder, where the states are either localised on the A or the B atoms, we obtain a $E(k)$ dispersion of the spectral function for A and B bands, which resembles that of an ordered AB crystal. Comparing our results with those of Ingers *et al* (1988) for the case of continuous disorder, we find that the spatial overlap between initial and final states becomes much more important in the case of chemical disorder. This is particularly true for large chemical disorder, where the A and B potentials become very different. In this case we find that only A–A and B–B transitions survive, and A–B transitions are suppressed. This leads to vanishing transition matrix elements for optical transitions between states close to the gap.

Comparison of our numerical results with the ones obtained from the CPA description shows that the latter gives a correct description of the principal effects of chemical disorder on the one-electron states as well as on the optical transition probabilities. This is encouraging, since it is well known that the CPA description becomes much better for the 2D and 3D case.

References

Abe S and Toyozawa Y 1981 *J. Phys. Soc. Japan* **50** 2185
Abrahams E, Anderson P W, Licciardello D C and Ramakrishnan T V 1979 *Phys. Rev. Lett.* **42** 673
Economou E N 1979 *Green's Functions in Quantum Physics, Springer Series in Solid State Sciences* vol 7 (Heidelberg: Springer)
Eggarter T P and Troper A 1987 *Phys. Status Solidi* b **140** 127
Ingers J, Maschke K and Proennecke S 1988 *Phys. Rev.* **37** 6105
Moullet I, Maschke K and Kunz H 1985 *J. Non-Cryst. Solids* **77/78** 17
Soven P 1967 *Phys. Rev.* **156** 809
—— 1969 *Phys. Rev.* **178** 1136
Velicky B 1969 *Phys. Rev.* **184** 614
Velicky B, Kirkpatrick S and Ehrenreich H 1968 *Phys. Rev.* **175** 747